Journal of Optoelectronics and Advanced Materials Vol. 6, No. 1, March 2004, p. 53 - 56

CONDUCTION MECHANISMS IN SILICON-BASED NANOCOMPOSITES

V. Iancu, M. Draghici[a], L. Jdira[a], M. L. Ciurea[*a]

University “Politehnica” of Bucharest, Bucuresti 77206, Romania
[a]National Institute of Materials Physics, Bucuresti-Magurele, 77125, Romania

Electrical conduction mechanisms in Si – SiO_2 nanocomposite films were experimentally investigated and theoretically modelled. The films with silicon volume concentration varying from 0 % to 100 % were deposited on rectangular quartz substrates. They were prepared by co-sputtering CVD from two targets, one of silicon and one of silicon dioxide. Their middle part is formed by Si nanodots embedded in SiO_2. 50 parallel aluminium electrodes were deposited, forming 49 coplanar samples, centred around x = 45 % Si concentration. The microstructure investigations proved that the silicon nanodots have diameters between 4 nm (x = 23 %) and 36 nm (x = 81 %). The current – voltage characteristics were measured at room temperature, in the – 25 ÷ + 25 V interval. The obtained curves are symmetric and superlinear. As the current – voltage characteristic is determined by the maximum resistance met by the carriers in their path, the experimental curve is modelled by the field-assisted tunnelling under Coulomb blockade. The used parameters are correlated with previous results obtained on nanocrystalline porous silicon. The correlation coefficient between the theoretical formula and the experimental data is greater than 99.95 %.

(Received September 9, 2003; accepted February 5, 2004)

Keywords: Silicon nanodots, Electrical transport, Quantum confinement

1. Introduction

The leading material in the ultra-large scale integrated electronics is the silicon. Integration and economy of scale are the two major elements for its technological success. 10^8 transistors and information transfer lengths of 15 km in a single chip are common today [1,2]. Low dimensional silicon presents a great interest for the scientific world because of both the quantum effects that confer it new properties and the possibility of using it in nano- and opto-electronics.

The first low dimensional silicon system intensely studied was the porous silicon (PS). The interest in PS was aroused by its photoluminescence in the visible range with high quantum efficiency at room temperature (RT) [3,4]. However, the hope of using PS in integrated optoelectronics could not be achieved because of the impossibility of calibrating the nanocrystals, and of the surface/interface effects that strongly interfere with the quantum processes [5-8].

The Si – SiO_2 nanocomposites partially surpass these troubles [9]. One can calibrate the nanodots, but the optical and electrical properties cannot be properly matched yet. One of the main problems to be studied in this context is that of the electrical transport. Several studies were made and different models were proposed to describe it. Among them were: (i) the hopping process at low temperatures and thermal activation at high temperatures [10], (ii) the Poole-Frenkel mechanism [11], (iii) the fractal percolation [12], (iv) the generation-recombination phenomena in the depletion region [13], (v) the dangling bonds [14], and (vi) thermally assisted tunnelling [15-17].

In this paper, the conduction mechanism in Si – SiO_2 nanocomposites is investigated. Section 2 presents the preparation and the current – voltage measurements. The model of the field assisted tunnelling under Coulomb blockade [18-20] is analyzed in Section 3. Section 4 discusses the experimental results in the frame of the model and the last Section presents the conclusions.

[*] Corresponding author: ciurea@alpha1.infim.ro

2. Experimental

Si – SiO_2 nanocomposite films were deposited by co-sputtering of Si and SiO_2. The targets are formed by two attached semicircles of Si and SiO_2. The quartz slide substrate, with a length of 13 cm, is located 5 cm above the targets. This configuration allows the deposition in a single run of a film with variable concentration of Si from practically x = 0 vol. % to practically x = 100 vol. %. The sputtering takes place in a pure (99.9995%) Argon atmosphere, at a pressure of 19 mTorr. The thickness of the films obtained after 12 h sputtering is 9 μm. The annealing of the films at 1100 °C for 30 min in a N_2 flow was necessary for the nucleation of crystallites. The samples for electrical measurements were prepared by evaporation of 50 parallel Al contacts in a coplanar configuration Each electrode has 7 mm long and the distance between two consecutive electrodes is 1 mm.

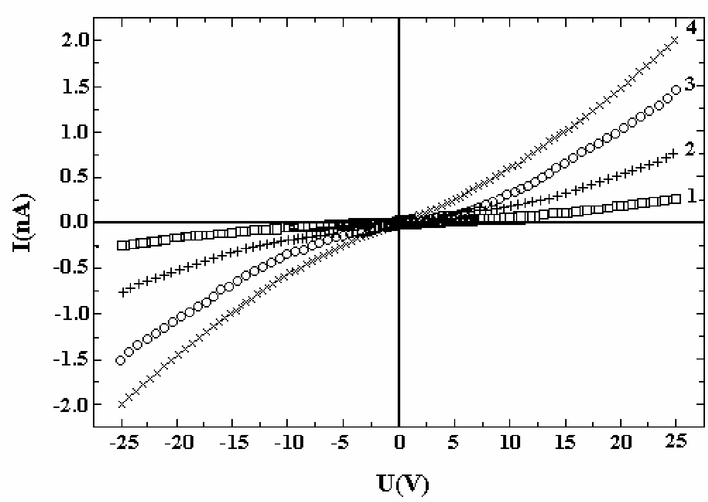

Fig. 1. Current – voltage characteristics: x_1 = 67 vol. %, x_2 = 69 vol. %, x_3 = 72 vol. %, and x_4 = 74 vol. %.

The current – voltage measurements were performed at room temperature (RT) using a Keithley 642 electrometer and an Agilent E3631A d.c. power supply. Fig. 1 illustrates the current – voltage characteristics of three samples with Si concentrations of 67, 69, 72 and 74 vol. %. As one can see, the curves are almost symmetric and superlinear.

3. Theoretical model

Two phenomena determine the electrical behaviour of the nanodots films: the carrier ballistic movement inside the nanodots and the transport between them, respectively. If the crystalline nanodots are embedded in a matrix, the transport between them depends on the matrix material. The carriers move mainly by tunnelling for insulating matrices. The current – voltage behaviour is determined by the maximum resistance part from the minimum resistance path. Therefore, the current – voltage characteristic is dominated by the tunnelling.

Due to the Coulomb blockade, one cannot find more than one non-compensate carrier inside a nanodot. The field assisted tunnelling under Coulomb blockade is described by the formula [18-20]

$$I = a\left[\varphi \exp\left(-\Delta s \cdot \chi\sqrt{\varphi}\right) - (\varphi + qU_b)\exp\left(-\Delta s \cdot \chi\sqrt{\varphi + qU_b}\right)\right], \tag{1}$$

where a is a proportionality constant, φ and Δs are the mean height and width of the potential barrier, and $\chi = \sqrt{8m^*/\hbar^2}$, m^* being the carrier effective mass. If the tunnelled barriers can be considered as roughly equal, $U_b = U/N$, where U is the bias applied to the sample and N the mean number of barriers.

Eq. (1) can be transcribed as

$$I = I_0 \cdot \mathrm{sign}(a) \cdot \mathrm{sign}(U) \cdot \left[\exp(-\alpha) - \left(1 + \mathrm{sign}(q) \frac{|U|}{U_0} \right) \exp\left(-\alpha \sqrt{1 + \mathrm{sign}(q) \frac{|U|}{U_0}} \right) \right], \qquad (2)$$

where $I_0 = |a| \cdot \varphi$, $U_0 = N \cdot \varphi / |q|$ and $\alpha = \Delta s \cdot \chi \sqrt{\varphi}$. $\mathrm{sign}(a) = \mathrm{sign}(q)$ because the current has the same sign with the bias. In addition, the super- or sub-linear character of the $I = I(U)$ curves is given by the charge sign. For super-linear curves, $q = -e$, where e is the elementary charge. Consequently, Eq. (2) becomes

$$I = I_0 \cdot \mathrm{sign}(U) \cdot \left[\left(1 - \frac{|U|}{U_0} \right) \exp\left(-\alpha \sqrt{1 - \frac{|U|}{U_0}} \right) - \exp(-\alpha) \right]. \qquad (3)$$

It results that one cannot determine all the four theoretical parameters (a, N, Δs, and φ), but only the fit parameters I_0, U_0 and α.

4. Results and discussion

Fig. 2 presents the fit of the experimental curves from Fig. 1 with the relation (3). The fit parameters are I_0 = 19.433 A, U_0 = 205.11 V, α = 25.844 for the first curve, I_0 = 5.157 A, U_0 = 195.16 V, α = 23.973 for the second, I_0 = 25.252 A, U_0 = 258.67 V, α = 24.333 for the third, and I_0 = 34.234 A, U_0 = 291.79 V, α = 24.132 for the fourth. For all the curves, the correlation coefficient is greater than 0.9995.

From previous measurements performed on nanocrystalline porous silicon it results that the height of the Si – SiO_x (x>1) potential barrier is φ = 2.2 eV [21]. If this value is considered as a good approximation for Si – SiO_2 barrier, then the parameters for the three curves are $N_1 \cong 93$, $N_2 \cong 89$, $N_3 = 118$, $N_4 \cong 133$, and $\Delta s_1 \cong \Delta s_2 \cong \Delta s_3 \cong \Delta s_4 \cong 1.6$ nm.

It has to be remarked that the mean number of tunnelled barriers N does not represent the whole electron path. The rest of the path is crossed by the electron through less resistive inter-particle junctions. This part of the path does not significantly influence the current – voltage characteristic [19].

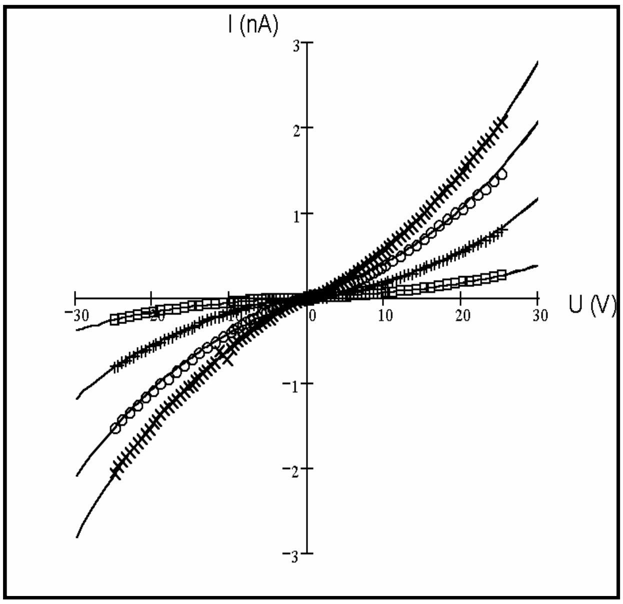

Fig. 2. Theoretical fit (solid lines) of the curves from Fig. 1 (: curve 1, +: curve 2, o: curve 3, ×: curve 4).

This general behaviour, obtained here in the coplanar configuration and the fact that similar behaviours have been found for non-rectifying contacts of Al in sandwich configuration [22] suggest that the non-linearity is associated with a bulk and not a contact effect.

5. Conclusions

Current – voltage characteristics measured in coplanar configuration on Si – SiO_2 nanocomposite films are symmetric and superlinear.

The theoretical modelling shows that the dominant conduction mechanism is the field assisted tunnelling under Coulomb blockade.

Acknowledgements

The authors are grateful to Prof. Isaac Balberg, Racah Institute of Physics, Hebrew University of Jerusalem, for the preparation of the samples and for helpful discussions.

References

[1] International Technology Roadmap for Semiconductors, 2000 Update, Interconnect (electronic document at http://public.itrs.net/).
[2] Silicon based microphotonics: from basics to applications, Ed. O. Bisi, S. U. Campisano, L. Pavesi, F. Priollo, I. O. S. Press, Amsterdam (1999).
[3] L. T. Canham, Appl. Phys. Lett. **57,** 1046 (1990).
[4] V. Lehmann, V. Gösele, Appl. Phys. Lett. **58,** 8621 (1991).
[5] Light emission in Silicon: From Physics to Devices, Ed. D. J. Lockwood, Academic Press, New York (1998).
[6] B. Hamilton, Semicond. Sci. Technol. **10,** 1187 (1995).
[7] A. G. Cullis, L. T. Canham, P. D. J. Calcott, J. Appl. Phys. **82**, 909 (1997).
[8] Properties of Porous Silicon, Ed. L. T. Canham, EMIS Datareviews Series No. 18, INSPEC, London (1997).
[9] M. Zacharias, J. Heitmann, R. Scholz, U. Kahler, M. Schmidt, J. Bläsing, Appl. Phys. Lett. **80**, 661 (2002).
[10] N. Koshida, H. Koyama, Mater. Res. Soc. Symp. Proc. **283,** 337 (1993).
[11] M. Ben-Chorin, F. Möller, F. Koch, Phys. Rev. B **49,** 2981 (1994).
[12] M. Ben-Chorin, F. Möller, F. Koch, Phys. Rev. B **51,** 2199 (1995).
[13] D. B. Dimitrov, Phys. Rev. B **51,** 1562 (1995).
[14] D. Stievenard, D. Deresmes, Appl. Phys. Lett. **67**, 1570 (1995).
[15] Y. L. He, X. N. Liu, Z. C. Wang, G. X. Cheng, L. C. Wang, S. D. Yu, Sci. China, Ser. A **36**, 248 (1993).
[16] G. Y. Hu, R. F. O'Connell, Y. L. He, M. B. Yu, J. Appl. Phys, **78,** 3945 (1995).
[17] Y. L. He, Y. Y. Wei, G. Z. Zhang, M. B. Yu, M. Liu, J. Appl. Phys. **82,** 3408 (1997).
[18] J. G. Simmons, J. Appl. Phys. **34**, 1793 (1963).
[19] M. Reshotko, A. Sa'ar, I. Balberg, phys. stat. sol. (a) **197**, 113 (2003).
[20] M. L. Ciurea, M. Draghici, V. Iancu, M. Reshotko, I. Balberg, J. Luminescence **102-103**, 492 (2003).
[21] M. L. Ciurea, I. Baltog, M. Lazăr, V. Iancu, S. Lazanu, E. Pentia, Thin Solid Films **325**, 271 (1998).
[22] T. A. Burr, A. A. Seraphin, E. Werwa, K. D. Kolenbrander, Phys. Rev. B **56**, 4818 (1997).